JACS
JOURNAL OF THE AMERICAN CHEMICAL SOCIETY

Subscriber access provided by ISTANBUL TEKNIK UNIV

Article

Hydrogen Bonding Effects on the Electronic Configuration of Five-Coordinate High-Spin Iron(II) Porphyrinates

Chuanjiang Hu, Bruce C. Noll, Paula M. B. Piccoli, Arthur J. Schultz, Charles E. Schulz, and W. Robert Scheidt

J. Am. Chem. Soc., **2008**, 130 (10), 3127-3136 • DOI: 10.1021/ja078222l

Downloaded from http://pubs.acs.org on February 8, 2009

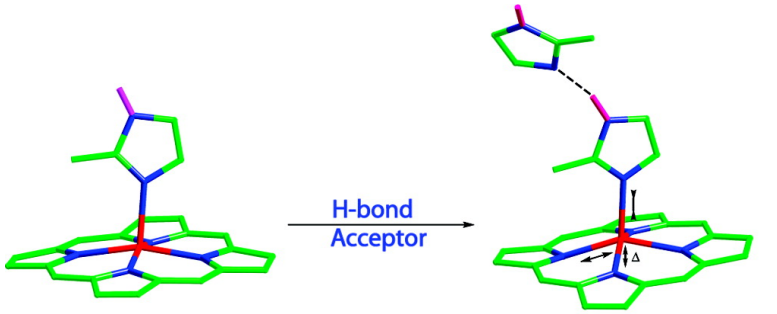

Imidazole imidazole or imidazolate?

More About This Article

Additional resources and features associated with this article are available within the HTML version:

- Supporting Information
- Links to the 2 articles that cite this article, as of the time of this article download
- Access to high resolution figures
- Links to articles and content related to this article
- Copyright permission to reproduce figures and/or text from this article

View the Full Text HTML

ACS Publications
High quality. High impact.

Journal of the American Chemical Society is published by the American Chemical Society. 1155 Sixteenth Street N.W., Washington, DC 20036

J|A|C|S
ARTICLES
Published on Web 02/14/2008

Hydrogen Bonding Effects on the Electronic Configuration of Five-Coordinate High-Spin Iron(II) Porphyrinates

Chuanjiang Hu,[†] Bruce C. Noll,[†] Paula M. B. Piccoli,[‡] Arthur J. Schultz,[‡] Charles E. Schulz,*[,§] and W. Robert Scheidt*[,†]

Department of Chemistry and Biochemistry, University of Notre Dame, Notre Dame, Indiana 46556, Intense Pulsed Neutron Source, Argonne National Laboratory, Argonne, Illinois 60439-4814, and Department of Physics, Knox College, Galesburg, Illinois 61401

Received October 26, 2007; E-mail: scheidt.1@nd.edu

Abstract: The characterization of a new five-coordinate derivative of (2-methylimidazole)(tetraphenylporphinato)iron(II) provides new and unique information about the effects of forming a hydrogen bond to the coordinated imidazole on the geometric and electronic structure of iron in these species. The complex studied has two crystallographically distinct iron sites; one site has an axial imidazole ligand modified by an external hydrogen bond, and the other site has an axial imidazole ligand with no external interactions. The iron atoms at the two sites have distinct geometric features, as revealed in their molecular structures, and distinct electronic structures, as shown by Mössbauer spectroscopy, although both are high spin ($S = 2$). The molecule with the external hydrogen bond has longer equatorial Fe−N_p bonds, a larger displacement of the iron atom out of the porphyrin plane, and a shorter axial bond compared to its counterpart with no hydrogen bonding. The Mössbauer features are distinct for the two sites, with differing quadrupole splitting and isomer shift values and probably differing signs for the quadrupole splitting as shown by variable-temperature measurements in applied magnetic field. These features are consistent with a significant change in the nature of the doubly populated d orbital and are all in the direction of the dichotomy displayed by related imidazole and imidazolate species where deprotonation leads to major differences. The results points out the possible effects of strong hydrogen bonding in heme proteins.

Introduction

Among the intriguing attributes of heme proteins is the wide range of physiological function carried out by these systems with the same prosthetic group, the iron derivative of protoporphyrin IX, commonly called heme. A particularly striking pair of heme protein families are the globins, whose biological function is the reversible transport and storage of dioxygen, and the peroxidases, enzymes that catalyze the conversion of hydrogen peroxide to water and/or the oxidation of substrates. One of the most intensively studied of the peroxidases is horseradish peroxidase (HRP), where the iron(II) HRP enzyme reacts irreversibly with dioxygen to form Compound III.[1] Despite this varied chemistry, both the globins and the peroxidases have a coordinated imidazole from a histidyl residue of the protein chain as the proximal ligand. However, it has been postulated that the histidine residue in HRP is strongly hydrogen bonded to a conserved aspartic acid that stabilizes higher oxidation states of iron and distinctly alters the chemical behavior of the peroxidases relative to the globins. The proximal imidazole in the globins also forms a hydrogen bond to a backbone carbonyl oxygen atom, a somewhat weaker hydrogen bond acceptor than that of the oxygen of aspartate. The importance of this hydrogen bond has been commented on and calculated on but, to our knowledge, has not been experimentally investigated in a systematic manner.

The crystal structures of heme proteins show that the occurrence of a hydrogen bond to a coordinated imidazole of a histidine residue is very widespread.[2−4] The strength of these hydrogen bonds are thought to vary from very weak proton donation to complete donation to form the imidazolate ligand.[5−9] There has been substantial speculation that hydrogen bonding in heme proteins could control the relative stability of the oxidation state of iron and even control reactivity of the heme protein.[10] In horseradish peroxidase,[11−12] the proximal histidine (His170) is ligated to the heme center and forms a hydrogen bond with a highly conserved aspartate group Asp247. The role

[†] University of Notre Dame.
[‡] Argonne National Laboratory.
[§] Knox College.

(1) Compound III is nominally equivalent to oxymyoglobin or -hemoglobin, so that the irreversible binding of O_2 in HRP demonstrates a significant difference between HRP and the globins.

(2) Zerić, S. D.; Popović, D. M.; Knapp, E.-W. *Biochemistry* **2001**, *40*, 7914.
(3) Valentine, J. S.; Sheridan, R. P.; Allen, L. C.; Kahn, P. *Proc. Natl. Acad. Sci. U.S.A.* **1979**, *76*, 1009.
(4) Salemme, F. R.; Freer, S. T.; Ng Huu Xuong Alden, R. A.; Kraut, J. *J. Biol. Chem.* **1973**, *248*, 3910.
(5) Peisach, J.; Blumberg, W. E.; Adler, A. *Ann. N. Y. Acad. Sci.* **1973**, *206*, 310.
(6) Nicholls, P. *Biochim. Biophys. Acta* **1962**, *60*, 217.
(7) Mincey, T.; Traylor, T. G. *J. Am. Chem. Soc.* **1979**, *101*, 765.
(8) Teroaka, J.; Kitagawa, T. *Biochem. Biophys. Res. Commun.* **1980**, *93*, 674.
(9) Morrison, M.; Schonbaum, G. R. *Annu. Rev. Biochem.* **1976**, *45*, 861.
(10) Peisach, J. *Ann. N. Y. Acad. Sci.* **1975**, *244*, 187.
(11) Berglund, G. I.; Carlsson, G. H.; Smith, A. T.; Szöke, H.; Henriksen, A.; Hajdu, J. *Nature* **2002**, *417*, 463.
(12) Gajhede, M.; Schuller, D. J.; Henriksen, A.; Smith, A. T.; Poulos, T. L. *Nat. Struct. Biol.* **1997**, *4*, 1032.

of this hydrogen bond is still one of the unresolved issues concerning peroxidase. A number of investigations have focused on this important issue. Most have been concerned about the high-valent Compound I active state.[13−17] It has been postulated that this strong hydrogen bond increases the basicity of the His170 proximal ligand relative to the globins, thus helping to stabilize the high oxidation state intermediates.[12] DFT calculations by Deeth[17] and Green[13] for the electronic structure of Compound I state(s) show some differences, but each predict a larger delocalization of the porphyrin radical onto imidazolate rather than imidazole for the Compound I intermediate. Furthermore, Green's calculation with the imidazolate-based radical can reproduce the small spin coupling constant between $S = 1$ iron-oxo unit and the $S = {}^1/_2$ radical. This is in agreement with an earlier NMR experiment[14] by La Mar and co-workers that implicated a porphyrin cation radical delocalized over the proximal histidine in Compound I. However, a recent hybrid quantum mechanical/molecular mechanical study[16] gave a different result that suggests the proximal ligand is imidazole rather than imidazolate.

There are a few studies on the nature of reduced HRP, which is a high-spin, five-coordinate iron(II) species. Electronic spectra[7] and resonance Raman spectra[8,18] have suggested the presence of deprotonated imidazole caused by the strong hydrogen bond to the aspartate. Reduced HRP was also studied by Mössbauer spectroscopy and compared with deoxymyoglobin.[19,20] These Mössbauer studies, in a strong magnetic field, showed remarkable differences between reduced HRP and deoxymyoglobin even though both are five-coordinate hemes with histidine as the axial ligand. Reduced HRP has a positive quadrupole splitting constant ($V_{zz} > 0$) and a rather small asymmetry value,[20] whereas deoxyMb has a large asymmetry constant and a negative value of the quadrupole splitting constant ($V_{zz} < 0$). This strongly argues for different properties of the axial ligand in the five-coordinate iron(II) states of reduced HRP and deoxy-Mb. By contrast, an ^{1}H NMR study by La Mar[21] suggests the proximal ligand in reduced HRP is an imidazole.

In an interesting investigation, Walker et al.[22] showed that forming a hydrogen bond to the N−H group of coordinated imidazole led to a substantial increase in the magnitude of the binding constant in the reaction shown in below.

$$[\mathrm{Fe(TPP)(Cl)}] + 2\mathrm{HIm} \rightleftharpoons [\mathrm{Fe(TPP)(HIm)_2}]^+ + \mathrm{Cl}^- \quad (1)$$

Thus, the formation of the bis-ligated iron(III) porphyrinate was enhanced by a factor of $\sim 10^3$ when the coordinated imidazoles were hydrogen bonded compared to no hydrogen bonding. Indeed, the formation of a stronger Fe−N(Im) bond was suggested to be the result of forming the hydrogen bonds. Balch and co-workers[23,24] subsequently showed that the equilibrium in the equation above was significantly shifted to the right by the addition of the hydrogen bond acceptor 1,10-phenanthroline. Balch et al. investigated this system by the use of visible spectroscopy and NMR studies. In the NMR experiment, diamagnetic cobalt(III) derivatives were substituted for the paramagnetic iron(III) center. Observed proton shifts are consistent with the formation of a hydrogen bond between imidazole and 1,10-phenanthroline. Finally, it had been previously reported that imidazolate is a stronger field ligand than imidazole.[25]

We are interested in the nature of five-coordinate iron(II) porphyrinates. Our previous work[26−28] reported the effects observed on the molecular and electronic structure when an imidazole ligand in five-coordinate iron(II) porphyrinate derivatives of the type [Fe(Por)(2-MeHIm)][29] is deprotonated. Both imidazole- and imidazol*ate*-ligated iron(II) porphyrinates exhibit an $S = 2$ (quintet) state, but the structural parameters of the coordination group are distinct with both axial and equatorial bond distances differences and large differences in the displacement of iron from the porphyrin plane. The differences in the Mössbauer spectra obtained in applied magnetic fields indicate that the doubly occupied orbital is different in the two classes. This change in the d-electron configuration is clearly consistent with all observed differing features of the two classes.

On the basis of our previous studies, further investigation on the model complex of H-bonding species will not only fill up the gap between imidazole- and imidazolate-ligated porphyrinates but also help us understand how H-bonds influence the molecular and electronic structure of those high-spin species and the role of hydrogen bonds in peroxidases.

In this paper, the first of our investigations of hydrogen bond formation with a coordinated imidazole in a high-spin iron(II) porphyrinate system, we report the formation of a relatively strong hydrogen bond in the derivative [Fe(TPP)(2-MeHIm)]$_2$·2-MeHIm. This species has two independent five-coordinate, high-spin iron(II) porphyrinate sites, one with a hydrogen bond to the imidazole and the second with a "neutral" imidazole ligand. This complex has been studied by X-ray and neutron diffraction studies as well as Mössbauer spectroscopy to assess the effects of hydrogen-bonded imidazole as a ligand. These studies show that there is a clear difference in the iron(II) electronic structure between the two iron sites, distinctions that can be attributed to the presence of a hydrogen bond to the coordinated imidazole in the one site.

(13) Green, M. T. *J. Am. Chem. Soc.* **2000**, *122*, 9495.
(14) Thanabal, V.; La Mar, G. N.; de Ropp, J. S. *Biochemistry* **1988**, *27*, 5400.
(15) de Ropp, J. S.; Thanabal, V.; La Mar, G. N.; *J. Am. Chem. Soc.* **1985**, *107*, 8268.
(16) Derat, E.; Cohn, S.; Shaik, S.; Altun, A.; Thiel, W. *J. Am. Chem. Soc.* **2005**, *127*, 13611.
(17) Deeth, R. J. *J. Am. Chem. Soc.* **1999**, *121*, 6074.
(18) Stein, P.; Mitchell, M.; Spiro, T. G. *J. Am. Chem. Soc.* **1980**, *102*, 7795.
(19) Debrunner, P. In *Iron Porphyrins* Part 3; Lever, A. B. P., Gray, H. B., Eds.; VCH Publishers Inc.; New York, 1983; Chapter 2.
(20) Champion, P. M.; Chiang, R.; Münck, E.; Debrunner, P.; Hager, L. P. *Biochemistry* **1975**, *14*, 4159.
(21) La Mar, G. N.; de Ropp, J. S. *J. Am. Chem. Soc.* **1982**, *104*, 5203.
(22) Walker, F. A.; Lo, M.-W.; Ree, M. T. *J. Am. Chem. Soc.* **1976**, *98*, 5552.
(23) Balch, A. L.; Watkins, J. J.; Doonan, D. J. *Inorg. Chem.* **1979**, *18*, 1228.
(24) The increase in imidazole binding constants upon the addition of 1,10-phenanthroline had been noted previously by Abbott and Rafson, but the origin of the effect not established. Abbott, E. H.; Rafson, P. A. *J. Am. Chem. Soc.* **1974**, *96*, 7378.
(25) (a) Landrum, J. T.; Reed, C. A.; Hatano, K.; Scheidt, W. R. *J. Am. Chem. Soc.* **1978**, *100*, 3232. (b) Landrum, J. T.; Hatano, K.; Scheidt, W. R.; Reed, C. A. *J. Am. Chem. Soc.* **1980**, *102*, 6729.
(26) Hu, C.; Roth, A.; Ellison, M. K.; An, J.; Ellis, C. M.; Schulz, C. E.; Scheidt, W. R. *J. Am. Chem. Soc.* **2005**, *127*, 5675.
(27) Hu, C.; Noll, B. C.; Schulz, C. E.; Scheidt, W. R. *J. Am. Chem. Soc.* **2005**, *127*, 15018.
(28) Hu, C.; An, J.; Noll, B. C.; Schulz, C. E.; Scheidt, W. R. *Inorg. Chem.* **2006**, *45*, 4177.
(29) The following abbreviations are used in this paper: Por, generalized porphyrin dianion; TPP, dianion of *meso*-tetraphenylporphyrin; T*p*-OCH_3-PP, dianion of *meso*-tetra-*p*-methoxyphenylporphyrin; TTP, dianion of *meso*-tetratolylporphyrin; TpivPP, dianion of α,α,α,α-tetrakis(*o*-pivalamidophenyl)porphyrin; Piv_2C_8P, dianion of α,α,5,15-[2,2′-(octanediamido)-diphenyl]-α,α,10-20-bis(o-pivalamidophenyl)porphyrin; Im, generalized imidazole; HIm, imidazole; 2-MeHIm, 2-methylimidazole; 1,2-Me_2Im, 1,2-dimethylimidazole; N_{ax}, nitrogen of axial ligand; N_p, porphyrinato nitrogen; C_b, porphyrin β carbon; Ct, the center of four porphyrinato nitrogen atoms.

Experimental Section

General Information. Chlorobenzene was washed with concentrated sulfuric acid and then with water until the aqueous layer was neutral, dried with $MgSO_4$, and distilled twice over P_2O_5 under argon. Hexanes were distilled over sodium benzophenone. Ethanethiol (Aldrich) was used as received. 2-Methylimidazole (Aldrich) was recrystallized from toluene/methanol and dried under vacuum. All other chemicals were used as received from Aldrich or Fisher. *meso*-Tetraphenylporphyrin (H_2TPP) was prepared according to Adler et al.[30] [Fe(TPP)Cl] was prepared according to a modified Adler preparation;[31] [Fe(TPP)]$_2$O was prepared from [Fe(TPP)Cl].[32] Mössbauer measurements were performed on a constant acceleration spectrometer at 4.2−298 K in zero field and at 4.2 K in 6 and 9 T fields and at 100, 200, and 250 K at 9 T using a superconducting magnet system (Knox College).

Synthesis of [Fe(TPP)(2-MeHIm)]$_2$·2-MeHIm. [Fe(II)(TPP)] was prepared by reduction of [Fe(TPP)]$_2$O (32 mg, 0.024 mmol) with ethanethiol (∼1 mL) in ∼6 mL of chlorobenzene. The chlorobenzene solution was stirred for 3 days, then transferred by cannula into a Schlenk flask containing excess 2-methylimidazole (17 mg, 0.20 mmol) and 2,4,6-collidine (0.25 mL), and stirred for another hour. X-ray quality crystals were obtained by liquid diffusion using hexanes as the nonsolvent in sealed 8 mm diameter glass tubes. The solid-state Mössbauer samples were made from 95% ^{57}Fe-enriched single crystals and then immobilized in Apiezon grease.

X-Ray Structure Determination. Single-crystal experiments were carried out on a Bruker Apex II system with graphite monochromated Mo−K α radiation ($\bar{\lambda} = 0.71073$ Å). A red crystal with the dimensions $0.28 \times 0.11 \times 0.05$ mm^3 was used for the structure determination. The crystalline sample was placed in inert oil, mounted on a glass pin, and transferred to the cold gas stream of the diffractometer. Crystal data were collected at 100 K. The structure was solved by direct methods and refined against F^2 using SHELXTL;[33,34] subsequent difference Fourier syntheses led to the location of all remaining non-hydrogen atoms. For the structure refinement, all data were used, including negative intensities. The asymmetric unit contains two independent porphyrin molecules and one fully occupied 2-methylimidazole solvate. All 2-methylimidazoles were found to be completely ordered. All non-hydrogen atoms were refined anisotropically. All hydrogen atoms (including those of the 2-methylimidazole solvate) were found in Fourier maps, and all coordinates and isotropic temperature factors were refined. Refined C−H distances range from 0.90 to 1.04 Å, N−H distances range from 0.81 to 0.85 Å, and temperature factors for all hydrogen atoms range from 0.02 to 0.07 Å^2. The program SADABS[35] was applied for the absorption correction. Complete crystallographic details, atomic coordinates, anisotropic thermal parameters, and hydrogen atom coordinates are given in the Supporting Information.

Neutron Data Collection and Refinement. Neutron diffraction data were obtained at the Intense Pulsed Neutron Source (IPNS) at the Argonne National Laboratory using the time-of-flight Laue single-crystal diffractometer (SCD).[36,37] At the IPNS, pulses of protons are accelerated into a depleted uranium target 30 times per second to produce pulses of neutrons by spallation. Exploiting the pulsed nature of the source, neutron wavelengths are determined by time-of-flight based on the de Broglie equation $\lambda = (\hbar/m)\cdot(t/l)$, where $\hbar$ is Planck's constant, m is the neutron mass, and t is the time-of-flight for a flight path l, so that the entire thermal spectrum of neutrons can be used. With two position-sensitive area detectors and a range of neutron wavelengths, a solid volume of reciprocal space is sampled with each stationary orientation of the sample and the detectors. The SCD has two ^{6}Li-glass scintillation position-sensitive area detectors, each with active areas of 15×15 cm^2 and a spatial resolution of <1.5 mm. One of the detectors is centered at a scattering angle of 75° and a crystal-to-detector distance of 23 cm, and the second detector is at 120° and 18 cm, respectively. Details of data collection and analysis procedures have been published previously.[38]

A red crystal, with approximate dimensions of $2 \times 1 \times 1$ mm^3 and a weight of 3 mg, was mounted in a quartz capillary and packed in place with quartz wool and then was glued into an aluminum holder that was mounted on the cold stage of a closed-cycle helium refrigerator cooled to 20 ± 1 K. For each setting of the diffractometer angles, data were stored in three-dimensional histogram form with coordinates x,y,t corresponding to horizontal and vertical detector positions and the time-of-flight, respectively. An auto-indexing algorithm[39] was used to obtain an initial orientation matrix from the peaks in three preliminary histograms measured for 60 min each. This unit cell matched the previously reported X-ray unit cell indicating that the neutron sample was the correct material. For intensity data collection, runs of between 7 and 8 h per histogram were initiated. Settings were arranged at χ and ϕ values suitable to cover at least one unique hemisphere of reciprocal space (Laue symmetry $\bar{1}$). With the above counting times, 22 histograms were completed in the 8 days available for the experiment. Bragg peaks in the recorded histograms were indexed and integrated using individual orientation matrices for each histogram to allow for any misalignment of the sample. Intensities were integrated about their predicted locations and were corrected for the Lorentz factor, the incident spectrum, and the detector efficiency. A wavelength-dependent spherical absorption correction was applied using cross sections from Sears[40] for the non-hydrogen atoms and from Howard et al.[41] for the hydrogen atoms (μ (cm^{-1}) = 1.146 + 0.728 λ). Symmetry-related reflections were not averaged because different extinction factors are applicable to reflections measured at different wavelengths.

The GSAS software package was used for structural analysis.[42] The atomic positions of the X-ray diffraction structure were used as a starting point in the refinement. The refinement was based on F^2 reflections with a minimum d-spacing of 0.7 Å. Weights were assigned as $w(F_0^2) = 1/[(\sigma(F_0^2) + (F_0^2)]^2$, where $\sigma^2(F_0^2)$ is the variance based on counting statistics. Atoms were not able to be successfully refined with anisotropic parameters, even when employing rigid groups to assist with the data to parameter ratio. In the final refinement, all atoms, including hydrogen atoms, were refined freely with isotropic displacement parameters. After final refinement, the maximum peak of unmodeled scattering density in the difference Fourier map was 0.263 fm·Å^{-3}, which compares to approximately 8% of the peak height of atom N11 in a Fourier map. Data collection and refinement parameters for both the X-ray and neutron determinations are summarized in Table 1.

(30) Adler, A. D.; Longo, F. R.; Finarelli, J. D.; Goldmacher, J.; Assour, J.; Korsakoff, L. *J. Org. Chem.* **1967**, *32*, 476.

(31) (a) Adler, A. D.; Longo, F. R.; Kampus, F.; Kim, J. *J. Inorg. Nucl. Chem.* **1970**, *32*, 2443. (b) Buchler, J. W. In *Porphyrins and Metalloporphyrins*; Smith, K. M., Ed.; Elsevier Scientific Publishing: Amsterdam, The Netherlands, 1975; Chapter 5.

(32) (a) Fleischer, E. B.; Srivastava, T. S. *J. Am. Chem. Soc.* **1969**, *91*, 2403. (b) Hoffman, A. B.; Collins, D. M.; Day, V. W.; Fleischer, E. B.; Srivastava, T. S.; Hoard, J. L. *J. Am. Chem. Soc.* **1972**, *94*, 3620.

(33) Sheldrick, G. M. *SHELXTL*; Bruker-Nonius AXS: Madison, WI, 2001.

(34) $R_1 = \sum ||F_0| - |F_c||/\sum |F_o|$, $wR_2 = \{\sum[w(F_0^2 - F_c^2)^2]/\sum [w(F_0^2)^2]\}^{1/2}$ and $R(F^2) = \sum ||F_0|^2 - |F_c|^2|/\sum |F_0|^2$. The conventional R-factors R_1 are based on F, with F set to zero for negative F^2. The criterion of $F^2 > 2\sigma(F^2)$ was used only for calculating R_1. R-factors based on F^2 (wR_2) are statistically about twice as large as those based on F, and R-factors based on ALL data will be even larger.

(35) Sheldrick, G. M. *SADABS*; Universität Göttingen: Göttingen, Germany, 2006.

(36) Schultz, A. J.; Srinivasan, K.; Teller, R. G.; Williams, J. M.; Lukehart, C. M. *J. Am. Chem. Soc.* **1984**, *106*, 999.

(37) Schultz, A. J.; De Lurgia, P. M.; Hammonds, J. P.; Mikkelson, D. J.; Mikkelson, R. L.; Miller, M. E.; Naday, I.; Peterson, P. F.; Parker, R. R.; Worlton, T. G. *Phys. B* **2006**, *385−386*, 1059.

(38) Schultz, A. J.; Van, Derveer, D. G.; Parker, D. W.; Baldwin, J. E. *Acta Cryst. C* **1990**, *46*, 276.

(39) Jacobson, R. A. *J. Appl. Cryst.* **1976**, *19*, 283.

(40) Sears, V. F. In *Methods of Experimental Physics*, Vol. 23, Neutron Scattering, Part A. ed.; Academic Press: Orlando, FL, 1986; p 521−550.

(41) Howard, J. A. K.; Johnson, O.; Schultz, A. J.; Stringer, A. M. *J. Appl. Cryst.* **1987**, *20*, 120−122.

(42) Larson, A. C.; Von Dreele, R. B. *General Structure Analysis System−GSAS*; Los Alamos National Laboratory: Los Alamos, NM, 2000.

Table 1. Brief X-ray and Neutron Crystallographic Data and Data Collection Parameters

diffraction method	X-ray	neutron
formula	$C_{100}H_{74}Fe_2N_{14}$	
FW, amu	1583.43	
a, Å	13.1854(2)	13.176(7)
b, Å	17.5883(3)	17.570(7)
c, Å	19.0189(3)	19.06(1)
α, deg	111.751(1)	111.95(4)
β, deg	100.371(1)	100.34(5)
γ, deg	95.742(1)	95.84(4)
V, Å^3	3962.00(11)	3956(4)
space group	$P\bar{1}$	
Z	2	
D_c, g/cm^3	1.327	
F(000)	1648	
μ, cm^{-1}	4.27	$1.146 + 0.728\lambda$
crystal dimensions, mm	$0.28 \times 0.11 \times 0.05$	$2 \times 1 \times 1$
radiation	Mo-K α, $\bar{\lambda} = 0.71073$ Å	neutrons
temperature, K	100(2)	20(1)
total data collected	68673	4904
absorption correction	semiempirical from equivalents	wavelength-dependent spherical
unique data	16176 ($R_{int} = 0.050$)	
unique observed data	12597 [$I > 2\sigma(I)$]	2860 [$I > 3\sigma(I)$]
refinement method	Full-matrix least-squares on F^2	
final *R* indices	$R_1 = 0.0368$, $wR_2 = 0.0865$ [$I > 2\sigma(I)$]	$R(F^2) = 0.165$, $wR_2 = 0.171$ [$I > 3\sigma(I)$]
final *R* indices (all data)	$R_1 = 0.0552$, $wR_2 = 0.0944$	

Results

A new crystalline phase of the molecular species [Fe(TPP)(2-MeHIm)], [Fe(TPP)(2-MeHIm)]$_2$·2-MeHIm, was obtained during attempts to obtain a bulk sample of the previously reported five-coordinate iron(II) porphyrinate [Fe(TPP)(2-MeHIm)]·1.5C_6H_5Cl[43] for additional Mössbauer study. An extensive and eventually successful effort was made to reproduce the preparation and get a reliable bulk preparation, since this new imidazole solvate phase had unusual features that were expected to lead to interesting physical properties.

Molecular Structures. X-ray crystallography shows that the asymmetric unit of [Fe(TPP)(2-MeHIm)]$_2$·2-MeHIm contains two independent porphyrin molecules and one 2-methylimidazole solvate molecule. Both porphyrin molecules (molecules **1** and **2**) are five-coordinate imidazole-ligated iron(II) complexes. ORTEP diagrams showing both molecules are provided in Figure 1. In this figure and all tables, the following atom naming convention has been used: *Q*(*nyy*), where *Q* is the atom type, *n* refers to molecule **1** or **2** and *yy* are further numbers and letters needed to completely specify the atom. Thus similar atoms in the two molecules have the same name except for the digit *n*. Both 2-methylimidazole ligands and the solvate are completely ordered.

The displacement of each porphyrin core atom from the N_4 mean plane is shown in the formal diagrams of Figure 2. The orientation of the 2-methylimidazole ligand including the value of the dihedral angle is also shown; the circle represents the position of the methyl group. The absolute ligand orientation, given by the dihedral angle between the axial ligand plane and the closest $N_{ax}FeN_p$ plane and conventionally denoted by ϕ, is also shown. The ligand planes make dihedral angles of 16.0 and 22.9° to the closest $N_{ax}FeN_p$ plane in molecules **1** and **2**, respectively. Also included on the diagrams of Figure 2 are the individual Fe−N_p bond lengths. An analogous diagram showing atomic displacements from the 24-atom mean plane is given in Figure S1 (Supporting Information).

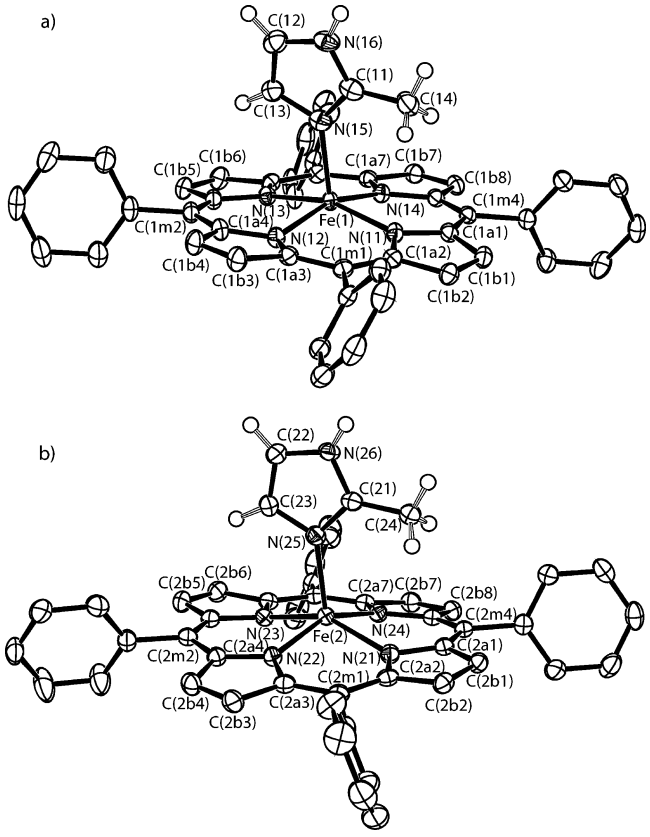

Figure 1. ORTEP diagrams of the two independent molecules in [Fe(TPP)(2-MeHIm)]$_2$·2-MeHIm. The atom labeling scheme for the axial ligand and the core atoms are shown. The hydrogen atoms of the porphyrin ligands have been omitted to improve clarity; 50% probability ellipsoids are depicted. (a) Molecule **1**. (b) Molecule **2**.

The dihedral angle between the imidazole ligand and the porphyrin plane is 79.7° in molecule **1** and 89.4° in molecule

(43) Ellison, M. K.; Schulz, C. E.; Scheidt, W. R. *Inorg. Chem.* **2002**, *41*, 2173.

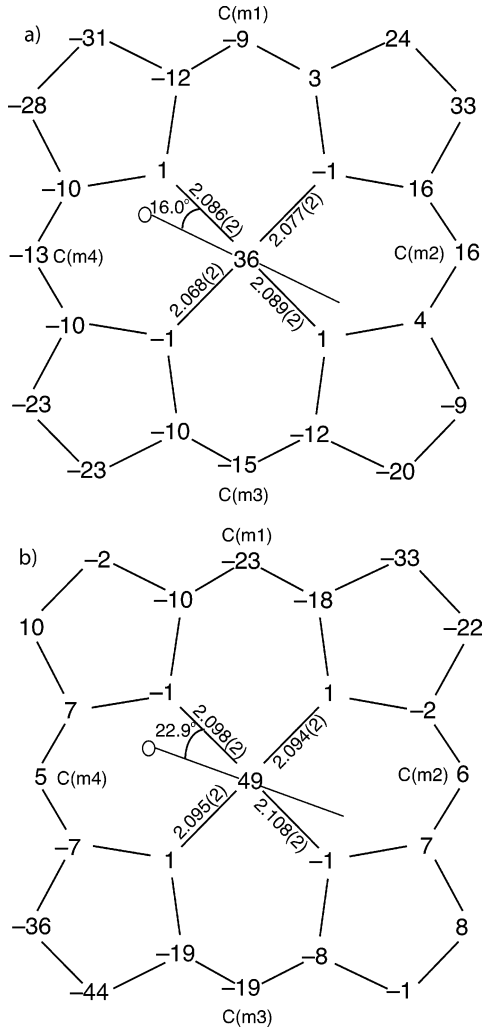

Figure 2. Diagrams illustrating the core conformation and iron displacement for both molecules in [Fe(TPP)(2-MeHIm)]$_2$·2-MeHIm. The displacement of the iron and the atoms of the porphyrin core from the mean plane defined by the four porphyrin nitrogen atoms is given in units of 0.01 Å. The position of the imidazole ligand with respect to directions defined by the Fe−N_p directions is shown. (a) Molecule **1**. (b) Molecule **2**. The position of the 2-methyl group of the coordinated ligand is shown by the small circle.

2. In molecule **1**, the average Fe−N_p distance is 2.080(9) Å, and the Fe−N_{Im} distance is 2.120(2) Å. In molecule **2**, the corresponding distances are 2.099(6) and 2.099(2) Å. In both molecules, the imidazole ligand Fe−N bond vector is tilted off of the normal to the 24-atom porphyrin mean plane. The value of the tilt angle, θ, is 9.2° for molecule **1** and 7.6° for molecule **2**. The radii of the central hole, given by Ct···N, are 2.050 and 2.040 Å, respectively, for molecules **1** and **2**.

All hydrogen atoms in the structure were located in difference Fourier maps. The collected X-ray data are quite extensive, and thus, all hydrogen atoms were treated as independent atoms with the three crystallographic coordinates and an isotropic temperature factor varied in the refinements. The experimentally derived C−H and N−H distances are quite reasonable with relatively small distance ranges. The ranges observed (average) are C_{phenyl}−H, 0.91(2)−1.04(3) Å (0.96(3) Å); C_b−H, 0.90(2)−0.99(2) Å (0.95(3) Å); C_{Im}−H, 0.93(2)−1.03(3) Å (0.97(3) Å); and N_{Im}−H, 0.81(3)−0.85(3) Å (0.83(2) Å). A complete listing of bond distances and angles for both molecules is given in the Supporting Information.

A 20 K neutron diffraction study for the complex has also been performed to verify hydrogen atom positions. Owing to the large size of the unit cell, the number of data are somewhat limited and atoms were refined with isotropic thermal parameters. The results, however, are in complete accord with the X-ray diffraction study. The N−H distances are 1.01(4) Å for N(16)−H(16) in molecule **1**, 1.06(3) Å for N(26)−H(26) in molecule **2**, and 1.05(5) Å for N(2S)−H(2NS) in the solvate.

Mössbauer Spectra. The crystalline species was studied with variable temperature Mössbauer spectroscopy from 4 to 298 K. The observed spectra consist of two quadrupole doublets with equal area and, as will be discussed later, can be assigned to the two independent iron sites of the crystalline derivative. Both quadrupole doublets show a strong temperature dependence. Mössbauer parameters at various temperatures are given in Table S2 of the Supporting Information.

Discussion

[Fe(TPP)(2-MeHIm)] Phases. The new crystalline phase of [Fe(TPP)(2-MeHIm)], [Fe(TPP)(2-MeHIm)]$_2$·2-MeHIm, was originally obtained during attempts to obtain a new bulk sample of the previously reported chlorobenzene solvate [Fe(TPP)(2-MeHIm)]·1.5C_6H_5Cl[43] for additional Mössbauer study. The original crystal preparation procedure now appears to yield at least two distinct crystalline species, [Fe(TPP)(2-MeHIm)]$_2$·2-MeHIm and [Fe(TPP)(2-MeHIm)]·1.5C_6H_5Cl.[44] The new imidazole solvate had unusual features that were expected to lead to interesting physical properties, and an extensive effort was made to reproducibly prepare this new phase. A variety of reaction conditions (concentration of metalloporphyrin and/or 2-methylimidazole, different solvents and bases) were attempted. Polymorphism or pseudopolymorphism appears to be a serious problem in ensuring that a characterization sample is a pure phase. In addition to the two phases above, crystals of composition [Fe(TPP)(2-MeHIm)]$_2$·2-MeHIm·C_6H_5Cl and [Fe(TPP)(2-MeHIm)]$_2$·0.5(C_6H_5Cl)[46] were obtained in some experiments. The desired crystalline phase can be produced if the hindered base 2,4,6-collidine is added to the crystallization solution. This procedure was used to prepare several large crystals for the neutron diffraction study. To get enough of the correct phase for Mössbauer study, 95% ^{57}Fe-enriched samples were also prepared. The ^{57}Fe-enriched crystals had the desired unit cell. Two ^{57}Fe crystalline samples have been measured by Mössbauer spectroscopy after unit cell checks of many crystals. Unit cell constants for alternative phases are given in ref 47. The air-sensitivity of the crystalline material necessitated the use of capillaries for the unit cell checks, and hence, only a

(44) The preservation of a few crystallizing tubes used in the early investigations reported in ref 43 and in single-crystal nuclear resonance vibrational studies (ref 45) and several prepared subsequent to those experiments support the idea that early crystallization experiments provided a single phase whereas later experiments provided two distinct phases. (All of these experiments were carried out by M.K.E., the later experiment by C.H. agree with the last experiments of M.K.E.)

(45) Rai, B. K.; Durbin, S. M.; Prohofsky, E. W.; Sage, J. T.; Ellison, M. K.; Scheidt, W. R.; Sturhahn, W.; Alp, E. E. *Phys. Rev. E* **2002**, *66*, 051904−1−12.

(46) Hu, C.; Scheidt, W. R. Unpublished observations.

(47) Unit cell constants for [Fe(TPP)(2-MeHIm)]·1.5C_6H_5Cl:[43] a = 12.334(3) Å, b = 13.515(6) Å, c = 14.241(7) Å, α = 70.62(3)°, β = 88.29(2)°, γ = 88.24(3)°, V = 2238(2) Å^3; for [Fe(TPP)(2-MeHIm)]$_2$·2-MeHIm)]·C_6H_5-Cl: a = 13.3632(4) Å, b = 17.1128(6) Å, c = 20.2999(7) Å, α = 73.498-(2)°, β = 80.289(2)°, γ = 89.301(2)°, V = 4384.1(3) Å^3; for and [Fe(TPP)(2-MeHIm)]$_2$·0.5(C_6H_5Cl): a = 17.904(4) Å, b = 10.151(2) Å, c = 23.061(5) Å, α = 90.00°, β = 108.47(3)°, γ = 90.00°, V = 3975.2-(14) Å^3.

Table 2. Comparisons of the Two Fe Sites of $[Fe(TPP)(2\text{-MeHIm})]_2 \cdot 2\text{-MeHIm}$

All X-Ray Data			
molecule 1		molecule **2**	
bond	length(Å)	bond	length (Å)
Fe(1)−N(11)	2.0860(15)	Fe(2)−N(21)	2.0983(15)
Fe(1)−N(12)	2.0766(15)	Fe(2)−N(22)	2.0937(16)
Fe(1)−N(13)	2.0894(15)	Fe(2)−N(23)	2.1083(15)
Fe(1)−N(14)	2.0683(15)	Fe(2)−N(24)	2.0951(15)
Fe(1)−N_p[a]	2.080(8)	Fe(2)−N_p[a]	2.099(7)
Fe(1)−N(15)	2.1205(17)	Fe(2)−N(25)	2.0993(16)
angle	value (deg)	angle	value (deg)
C(11)−N(15)−Fe(1)	131.55(14)	C(21)−N(25)−Fe(2)	128.96(13)
C(13)−N(15)−Fe(1)	122.44(13)	C(23)−N(25)−Fe(2)	125.72(13)
displacement	value (Å)	displacement	value (Å)
ΔN_4[b]	0.36	ΔN_4[b]	0.49
Δ[c]	0.41	Δ[c]	0.55

[a] Averaged value. [b] Displacement of iron from the mean plane of the four pyrrole nitrogen atoms. [c] Displacement of iron from the 24-atom mean plane of the porphyrin core.

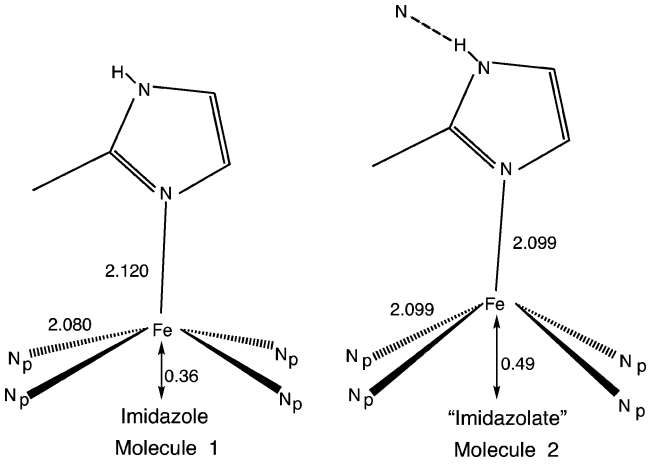

Figure 3. Schematic diagram comparing the FeN_5 coordination group geometries of molecule **1** (left) and molecule **2** (right). All distances are in Å.

selection of crystals in the Mössbauer sample could be reasonably checked. The Mössbauer samples are believed to consist of only the desired phase.

Molecular Structures. The two molecules shown in Figure 1 have the common features expected for five-coordinate high-spin iron(II) porphyrinates, including large equatorial Fe−N_p bond distances and a significant out-of-plane displacement of the iron(II) atom.[26,48] Although both molecules in the crystal are clearly five coordinate and high spin, there are significant, interesting, and unexpected differences between them. Selected structural parameters for the two molecules are listed in Table 2 and shown schematically in Figure 3. As can be seen from the table, the equatorial Fe−N_p bond distances and the out-of-plane displacements of molecule **1** are smaller than those of molecule **2**, whereas the axial bond distance is smaller for molecule **2**. The data in Table 2 and Figure 3 can be summarized as follows: In general, the structural features of molecule **1** are typical of those of other five-coordinate high-spin imidazole-ligated species,[26,28] whereas those of molecule **2** are much different. But, the structural differences between molecule **1** and **2** are strongly reminiscent of the differences between imidazole- and imidazolate-ligated high-spin iron porphyrins.[26] This can readily be seen from the structural data for molecules **1** and **2** given in Table 3 along with the comparable information for related species of the two types. The structural parameters for molecule **1** are dead-on with the average values of Fe−N_p, Fe−N_{im}, Δ N_4, and Δ previously found for eight different high-spin imidazole-ligated iron(II) derivatives. The corresponding parameters for molecule **2** are shifted so as to be substantially similar to those of the averaged values of the three imidazolate-ligated derivatives given in Table 3.

What causes the remarkable difference between the two molecules in $[Fe(TPP)(2\text{-MeHIm})]_2 \cdot 2\text{-MeHIm}$? An examination of the crystal environment and crystal packing strongly suggests the explanation. Figure 4 shows the immediate surroundings of both molecules in the crystalline lattice. There is a strong hydrogen bond between the coordinated imidazole of molecule **2** and the imidazole solvate molecule with an N(26)−N(1S) distance of 2.824(2) Å. The immediate question for this hydrogen bond is the location of the hydrogen atom that would ordinarily be associated with the coordinated imidazole. Is the imidazole ligand acting a hydrogen bond donor? Or has the proton been transferred to the acceptor? Otherwise put, which of the two possible representations for the hydrogen bond pair best depicts the situation: (i) a 2-MeHIm···2-MeHIm pair or (ii) a $2\text{-MeIm}^-/2\text{-MeH}_2\text{Im}^+$ pair?

The location of the hydrogen atoms associated with each imidazole in the X-ray structural results was very clear: each imidazole has one N−H group, with a normal (X-ray) N−H distance (N(16)−H(16) = 0.81(3) Å, N(26)−H(26) = 0.84(2) Å, and N(2S)−H(2NS) = 0.85(3) Å).[49] To further confirm the hydrogen atom position in the hydrogen bond, a neutron structure study has been performed at the Intense Pulsed Neutron Source at Argonne National Laboratory. In the neutron structure, which is somewhat limited in accuracy owing to the large triclinic unit cell and a relatively small number of reflections, the N(26)−H(26) distance (1.06(3) Å) in molecule **2** is only slightly longer the N(16)−H(16) distance (1.01(4) Å) in molecule **1**. Within the limits of the neutron diffraction experiment, all imidazole N−H distances are normal[50] and not statistically different: the N−H hydrogen atom of the coordinated imidazole has not been transferred. Figure 5 displays all of the hydrogen atom positions as determined from the neutron diffraction study. This diagram has a similar orientation of the two molecules to that given in Figure 4. We can thus conclude that the differences in the coordination geometry at iron in molecule **2** are the result of a hydrogen-bonded coordinated imidazole and not a coordinated imidazolate and is best described as a 2-MeHIm···2-MeHIm pair.

Because molecule **2** of this complex appears to show effects resulting from hydrogen bonding, a detailed understanding of its hydrogen bonding is of significant interest because of the hypothesis that hydrogen bonding to proximal ligands in hemoproteins can have substantial effects on the properties of the heme prosthetic group. The first question to be addressed

(48) Scheidt, W. R.; Reed, C. *A. Chem. Rev.* **1981**, *81*, 543.

(49) N−H distances from an X-ray analysis will be shorter than those found in a neutron diffraction experiment owing to the known foreshortening. Glusker, J. P.; Lewis, M.; Rossi, M. *Crystal Structure Analysis for Chemists and Biologists*; VCH Publishers, Inc.: New York, 1994; Chapter 9, p 376.

(50) The average N−H distances in Cambridge Structural Data Base from neutron diffraction studies is 1.023(57) Å.

Table 3. Selected Structural Parameters for [Fe(TPP)(2-MeHIm)]$_2$·2-MeHIm and Related Species[a]

complex[b]	Fe–N_p[c,d]	Fe–N_{1m}[d]	ΔN_4[d,e]	Δ[d,f]	Ct···N[d]	Fe–N–C[g,h]	Fe–N–C[g,i]	θ[g,j]	θ[g,k]	ref
[Fe(TPP)(2-MeHIm)] (Mol. **1**)	2.080(8)	2.120(2)	0.36	0.41	2.050	131.6(1)	122.4(1)	9.2	16.0	tw
[Fe(TPP)(2-MeHIm)] (Mol. **2**)	2.099(7)	2.099(2)	0.49	0.55	2.040	129.0(1)	125.7(1)	7.6	22.9	tw
[Fe(TPP)(1,2-Me_2Im)]	2.079(8)	2.158(2)	0.36	0.42	2.048	129.3(2)	124.9(2)	11.4	20.9	26
[Fe(TTP)(2-MeHIm)]	2.076(3)	2.144(1)	0.32	0.39	2.050	132.8(1)	121.4(1)	6.6	35.8	26
[Fe(Tp-OCH_3PP)(2-MeHIm)]	2.087(7)	2.155(2)	0.39	0.51	2.049	130.4(2)	123.4(2)	8.6	44.5	26
[Fe(Tp-OCH_3PP)(1,2-Me_2Im)]	2.077(6)	2.137(4)	0.35	0.38	2.046	131.9(3)	122.7(3)	6.1	20.7	26
[Fe(TPP)(2-MeHIm)](2-fold)	2.086(8)	2.161(5)	0.42	0.55	2.044	131.4(4)	122.6(4)	10.3	8.6	51
[Fe(TPP)(2-MeHIm)]·1.5C $_6H_5Cl$	2.073(9)	2.127(3)	0.32	0.38	2.049	131.1(2)	122.9(2)	8.3	24.0	43
[Fe(OEP)(1,2-Me_2Im)]	2.080(6)	2.171(3)	0.37	0.45	2.047	132.7(3)	121.4(2)	3.8	10.5	28
[Fe(OEP)(2-MeHIm)]	2.077(7))	2.135(3)	0.34	0.46	2.049	131.3(3)	122.4(3)	6.9	19.5	28
average of the eight	2.080(5)	2.147(16)	0.36(3)	0.44(6)	2.048(2)	131.4(12)	122.7(11)	7.8(24)		
[K(222)][Fe(OEP)(2-$MeIm^-$)]	2.113(4)	2.060(2)	0.56	0.65	2.036	136.6(2)	120.0(2)	3.6	37.4	27
[K(222)][Fe(TPP)(2-$MeIm^-$)]	2.118(13)	1.999(5)	0.56	0.66	2.044	129.6(3)	126.7(3)	9.8	23.4	27
		2.114(5)				133.6(4)	121.9(4)	6.5	21.6	
[Fe(TpivPP)(2-$MeIm^-$)]$^-$	2.11(2)	2.002(15)	0.52	0.65	2.045	NR[m]	NR	5.1	14.7	52
average of the three	2.114(4)	2.044(54)	0.55(2)	0.65(1)	2.042(5)					

[a] Estimated standard deviations are given in parentheses. [b] All complexes are high spin. [c] Averaged value. [d] In Å. [e] Displacement of iron from the mean plane of the four pyrrole nitrogen atoms. [f] Displacement of iron from the 24-atom mean plane of the porphyrin core. [g] Value in degrees. [h] 2-carbon, methyl substituted. [i] Imidazole 4-carbon. [j] Off-axis tilt (deg) of the Fe−N^b bond from the normal to the porphyrin plane. [k] Dihedral angle between the plane defined by the closest N_p−Fe−N_{Im} and the imidazole plane in deg. [l] Major imidazole orientation. [m] Not reported.

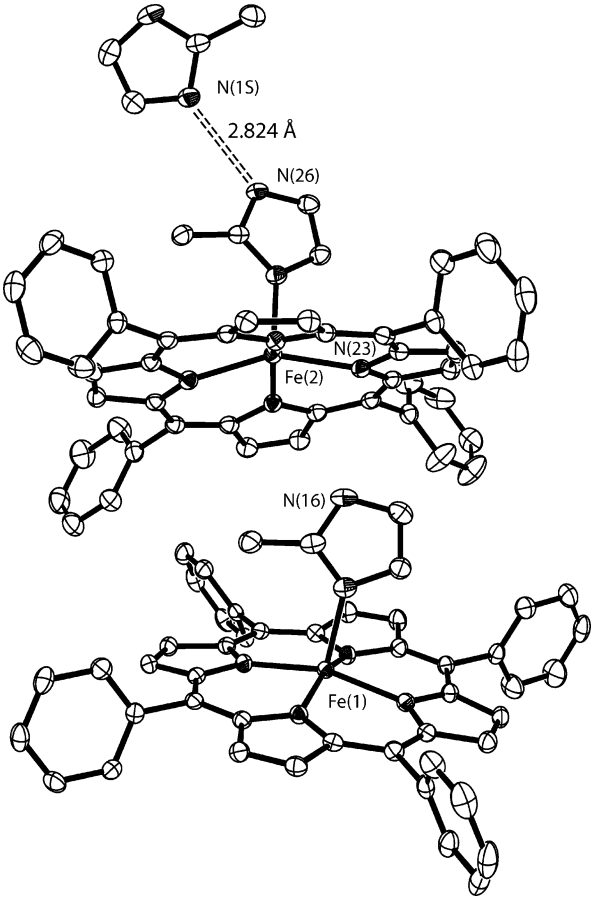

Figure 4. ORTEP diagram, based on the X-ray diffraction structure, showing the relative position of molecule **1** (bottom) and molecule **2** (top) in a portion of the unit cell. The close approach of the coordinated imidazole of molecule **2** with the imidazole solvate is shown. All atoms are contoured at the 50% probability level. For clarity, no hydrogen atoms are shown in this figure, but they are shown in Figure 5. The closest interatomic approach of the N(16) hydrogen atom is to N(23) with an N(16)···N(23) distance of 3.09 Å.

is the strength of the hydrogen bond in molecule **2**. As noted, the change (if any) in the length of the N−H bond cannot be accurately assessed from the neutron study, but it is clearly not exceptionally large. The neutron structural values are N(26)−H(26) = 1.059(33) Å, H(26)···N(1S) = 1.801(29) Å, with an

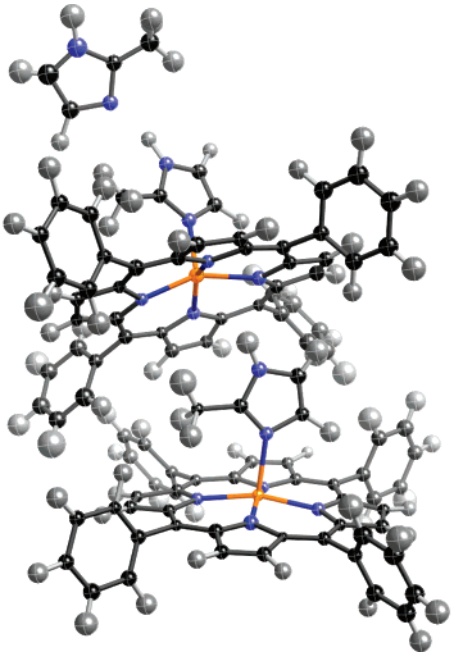

Figure 5. Thermal ellipsoid plot of [Fe(TPP)(2-MeHIm)]$_2$·2-MeHIm from the neutron diffraction structure; 50% probability ellipsoids are depicted (all atoms were refined isotropically). The two molecules have a similar orientation to that shown in Figure 4. All hydrogen atoms of the structure with the experimentally defined temperature factors are displayed. Hydrogen bonds in the crystal: N(26)···N(1S) = 2.829(15) Å, N(26)−H(26) = 1.06-(3) Å, N(26)−H(26)···N(1S) = 163(2)°.

N(26)−H(26)···N(1S) angle of 163(2)°. The most useful descriptor is the N(26)···N(1S) distance of 2.829(15) Å; the analogous separation from the X-ray data is 2.824(2) Å. The most effective method available for assessing the strength of the hydrogen bond is through a comparison of the appropriate distances and angles.

Two different hydrogen-bonding comparisons appear interesting. One is with imidazole itself. Crystalline imidazole is known to form strong self-hydrogen bonds and very polar solvents are required for its dissolution. Several crystal structure determinations of imidazole have been carried out by both X-ray[53] and neutron[54] diffraction studies. In the most pertinent study for comparison, by neutron diffraction at 103 K, the distance

equivalent to H(26)···N(1S) was found to be 1.809 Å, and the distance equivalent to N(26)···N(1S) was 2.849 Å.[54a] Thus, the hydrogen bond found in the present iron complex is marginally stronger than the strong hydrogen bond found in imidazole itself.

A second comparison utilizes the Cambridge Structural Database[55] to assess hydrogen bonds formed by imidazole in a range of differing crystal structures. We found a total of 391 instances of a hydrogen bond formed by an imidazole derivative to a nitrogen atom acceptor in a solid-state structure. Because almost all of these are X-ray diffraction studies, the imidazole hydrogen atom positions are relatively uncertain. Thus, the only distance that can be compared is the N···N distance equivalent to N(26)···N(1S). The mean value from the CSD for this distance is 2.900 Å. We can conclude that the hydrogen bond formed in the [Fe(TPP)(2-MeHIm)]$_2$·2-MeHIm derivative is a strong hydrogen bond but one that is not truly exceptional. We can also conclude that the strength of the hydrogen bond that can lead to an "imidazolate-like" structure can be described as strong but not exceptional.

As can be seen in Figure 2, the two cores have somewhat different conformations. However, our previous studies have shown that there is not a *single* preferred core conformation for imidazole-ligated high-spin iron(II) complexes.[26,28] Core conformations have been analyzed by the normal structural decomposition (NSD) method provided by Shelnutt et al.[56] Table S1 (Supporting Information) lists the NSD out-of-plane displacements of known high-spin iron(II) porphyrinates ligated with a 2-methylimidazole or 1,2-dimethylimidazole axial ligand. Neither molecule **1** nor molecule **2** displays any unusual features when compared to the other derivatives listed in Table S1.

Mössbauer Spectra. The second and perhaps more interesting question is the issue of the electronic structure of iron at the two sites. The geometry around iron is different because of hydrogen-bonding effects—how different is the electronic structure of iron at the two sites? The only effective physical method available for studying this question for this high-spin iron(II) system is that of Mössbauer spectroscopy. The spectra are unfortunately complicated by the presence of the two iron centers, which leads to two overlapped spectra.

Mössbauer spectra were measured from 25 to 298 K in a 50 mT field and at 4.2, 100, 200, and 250 K in 6 or 9 T applied fields. The 50 mT experimental data, at all temperatures, can be fit to a set of four overlapped Lorentzian lines. Thus, the spectra consist of two overlapped quadrupole doublets; an example spectrum is illustrated in Figure S2 (Supporting Information). The two doublets would be expected to have equal areas for a crystalline species that shows 1:1 stoichiometry of the two components, and in fact they can be adequately fit when constrained to equal areas.

The choice of the two quadrupole split doublets as lines 1 and 4 and lines 2 and 3 yields the only consistent assignment of isomer shift (δ) and quadrupole splitting (ΔE_q) values. The alternate choice leads to improbable values for the isomer shifts for high-spin iron(II) species.[19] The quadrupole splitting and isomer shift values for lines 2 and 3 range from $\Delta E_q = 2.53$ mm/s and isomer shift (δ) = 0.92 mm/s at 25 K to 1.90 and 0.80 mm/s at 298 K. This is similar to those values observed for other imidazole-ligated species,[26] including the temperature dependence, although the ΔE_q values are at the upper end of the values previously observed.

Thus, the quadrupole doublet from the line pair 2 and 3 is assigned as that most likely arising from the molecule **1** component of the sample. The second experimental component is that of the line pair 1 and 4 and is assigned as arising from molecule **2**. What values might have been expected for the molecule **2** component if hydrogen bonding has an effect? Likely limits at the low end of expected values would be those observed for imidazole-ligated iron(II) species and those at the high end are those of imidazolate-ligated iron(II). The actual values at 25 K are 3.14 mm/s for ΔE_q and 0.98 mm/s for δ. Consistent with these expectations, the isomer shift and quadrupole splitting values observed are significantly higher than those previously seen for imidazole-ligated species[26,28,43,57,58] but somewhat lower than those observed for imidazolate ligation.[27,52] It is thus clear that hydrogen bonding to the coordinated imidazole in [Fe(TPP)(2-MeHIm)]$_2$·2-MeHIm does cause a significant change of the quadrupole splitting value.

The experimental quadrupole splitting data for the two components of [Fe(TPP)(2-MeHIm)]$_2$·2-MeHIm are plotted in Figure 6. The temperature-dependent ΔE_q's for several related high-spin iron(II) species (imidazole-ligated, deoxy-hemoglobin, reduced HRP, and imidazolate-ligated) are also given in the Figure. All are seen to display significant temperature dependence. This large temperature dependence of the quadrupole splitting is believed to be the result of the presence of close-lying excited states of the same or lower spin multiplicity and appears to be a general feature of all five-coordinate imidazole-ligated iron(II) porphyrinates. The larger ΔE_q values for molecule **2** are clearly evident.

Perhaps the most interesting pair for comparison are those of molecule **2** and reduced HRP. The proximal histidine of HRP is known to be hydrogen bonded to a conserved aspartic acid in the resting iron(III) oxidation state and is presumed to remain hydrogen bonded in reduced HRP. Table 4 shows a more complete comparison between the Mössbauer data observed for molecules **1** and **2** and several related species. The table shows that, in addition to the magnitude of the quadrupole splitting, the sign of the quadrupole splitting is an important distinction between imidazole- and imidazolate-ligated iron(II) species. Imidazole ligation leads to a negative value of the quadrupole splitting whereas imidazolate ligation leads to a positive sign for the quadrupole splitting.[27] This distinction in sign arises from a differing symmetry of the doubly occupied orbital, which in the imidazolate species has essentially pure d_{xy} character. This

(51) (a) Collman, J. P.; Kim, N.; Hoard, J. L.; Lang, G.; Radonovich, L. J.; Reed, C. A. *Abstracts of Papers*; 167th National Meeting of the American Chemical Society; Los Angeles, CA, April 1974; American Chemical Society: Washington, D. C., 1974. (b) Hoard, J. L. personal communication to W.R.S. In particular, Prof. Hoard provided a set of atomic coordinates for the molecule.
(52) Mandon, D.; Ott-Woelfel, F.; Fischer, J.; Weiss, R.; Bill, E.; Trautwein, A. X. *Inorg. Chem.* **1990**, *29*, 2442.
(53) (a) Martinez-Carrera, S. *Acta Crystallogr.* **1966**, *20*, 783. (b) Epstein, J.; Ruble, J. R.; Craven, B. M. *Acta Crystallogr. B* **1982**, *38*, 140.
(54) (a) McMullan, R. K.; Epstein, J.; Ruble, J. R.; Craven, B. M. *Acta Crystallogr. B* **1979**, *35*, 688. (b) Craven, B. M.; McMullan, R. K.; Bell, J. D.; Freeman, H. C. *Acta Crystallogr. B* **1977**, *33*, 2585.
(55) Allen, F. H. *Acta Crystallogr.* **2002**, *B58*, 380. Bruno, I. J.; Cole, J. C.; Edgington, P. R.; Kessler, M. C.; Macrae, F.; McCabe, P.; Pearson J.; Taylor R. *Acta Crystallogr.* **2002**, *B58*, 389.
(56) Jentzen, W.; Ma, J.-G.; Shelnutt, J. A. *Biophys. J.* **1998**, *74*, 753. Sun, L.; Shelnutt, J. A.: Program is available via the internet at http://jashel-n.unm.edu.
(57) Kent, T. A.; Spartalian, K.; Lang, G.; Yonetani, T.; Reed, C. A.; Collman, J. P. *Biochem. Biophys. Acta* **1979**, *580*, 245.
(58) Momenteau, M.; Scheidt, W. R.; Eigenbrot, C. W.; Reed, C. A. *J. Am. Chem. Soc.* **1988**, *110*, 1207.

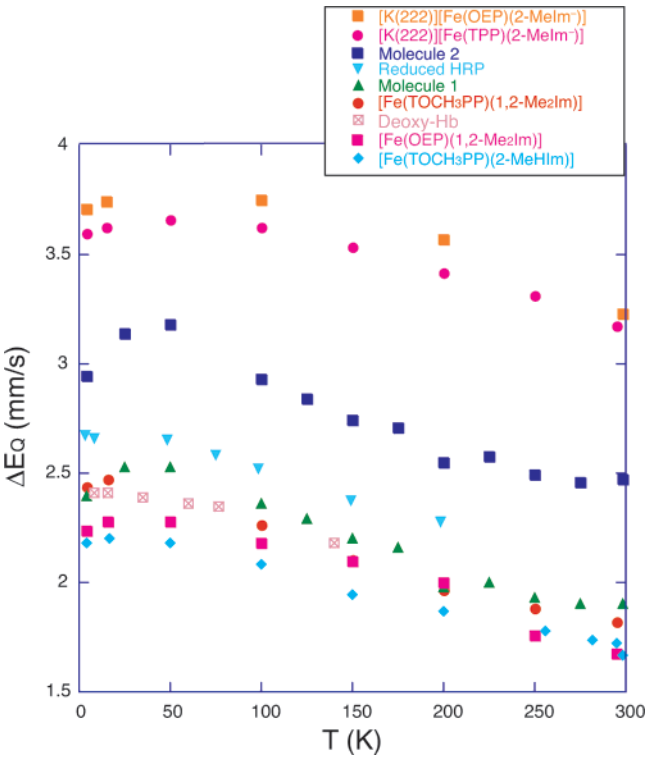

Figure 6. Plot of quadrupole splitting values as a function of temperature for molecules **1** and **2** and a number of related species. Species are identified in the order of the quadrupole splitting value. Data for [Fe(T*p*-OCH_3PP)-(2-MeHIm)] and [Fe(T*p*-OCH_3PP)(1,2-Me_2Im)] are from ref 26, those for [K(222)][Fe(OEP)(2-MeIm$^-$)] and [K(222)][Fe(TPP)(2-MeIm$^-$)] are from ref 27, those for [Fe(OEP)(1,2-Me_2Im)] are from ref 28, those for deoxy-Hb are from ref 57, and those for reduced HRP are from ref 59.

Table 4. Mössbauer Parameters for Five-Coordinate, High-Spin Imidazole-Ligated Iron(II) Porphyrinates

complex	ΔE_Q[a]	δ_{Fe}[a]	Γ[b]	*T*, K	ref
[Fe(TPP)(2-MeHIm)] (Mol. **1**)	|2.40|[c]	0.92	0.37	4.2	tw
[Fe(TPP)(2-MeHIm)] (Mol. **2**)	|2.90|[c]	0.97	0.58	4.2	tw
[Fe(Tp-OCH_3PP)(1,2-Me2Im)]	−2.44	0.95	0.46	4.2	26
[Fe(Tp-OCH_3PP)(2-MeHIm)]	−2.18	0.94	0.58	4.2	26
[Fe(TPP)(1,2-Me_2Im)]	−1.93	0.92	0.44	4.2	26
[Fe(TTP)(2-MeHIm)]	−1.95	0.85	0.42	4.2	26
[Fe(TTP)(1,2-Me_2Im)]	−2.06	0.86	0.43	4.2	26
[Fe(TPP)(2-MeHIm)]	−2.40	0.92	0.50	4.2	43
[Fe(TPP)(2-MeHIm)(2-fold)	−2.28	0.93	0.31	4.2	57
[Fe(TPP)(1,2-Me_2Im)]	−2.16	0.92	0.25	4.2	57
[Fe((Piv_2C_8P)(1-MeIm)]	−2.3[d]	0.88	0.40	4.2	58
[Fe(OEP)(1,2-Me_2Im)]	−2.23	0.92	0.37	4.2	28
[Fe(OEP)(2-MeHIm)]	−1.96	0.90	0.41	4.2	28
deoxy-Hb	−2.40	0.92	0.30	4.2	57
deoxy-Mb	−2.22	0.92	0.34	4.2	57
Reduced HRP	+2.70	0.90	0.38	4.2	59
K(222)[Fe(OEP)(2-MeIm$^-$)]	+3.71	1.00	0.31	4.2	27E
K(222)[Fe(TPP)(2-MeIm$^-$)]	+3.60	1.00	0.32	4.2	27
[Fe(TP_{piv}P)(2-MeIm)]$^-$	+3.51[e]	0.97		77	52
[Fe(OC_6H_5)(TPP)]$^-$	+4.01	1.03	0.38	4.2	60
[Fe(O_2CCH_3)(TP_{piv}P)]$^-$	+4.25	1.05	0.30	4.2	61
[Fe(OCH_3)(TP_{piv}P)]$^-$	+3.67[e]	1.03	0.40	4.2	62
[Fe(OC_6H_5)(TP_{piv}P)]$^-$	+3.90[e]	1.06	0.38	4.2	62
[$NaC_{12}H_{24}O_6$][Fe(TP_{piv}P)(SC_6HF_4)]	+2.38[e]	0.84	0.28	4.2	63
[Na(222)][Fe(T_{piv}PP)(SC_6HF_4)]	+2.38[e]	0.83	0.32	4.2	63
[Fe(T_{piv}PP)(SC_6H_5)]$^-$	+2.18	0.83	0.30	4.2	63
[Fe(T_{piv}PP)Cl]$^-$	+4.36[e]	1.01	0.31	77	64

[a] Units: mm/s. [b] Line width, fwhm. [c] Sign provisionally established, see text. [d] Sign not determined experimentally, presumed negative. [e] Sign not determined experimentally, presumed positive.

appears to be the usual electronic state for high-spin iron(II), whereas imidazole-ligated species, including deoxyhemoglobin and deoxymyoglobin, have a very low symmetry orbital comprised of a hybrid d_{xy}, d_{xz}, and d_{yz} set.

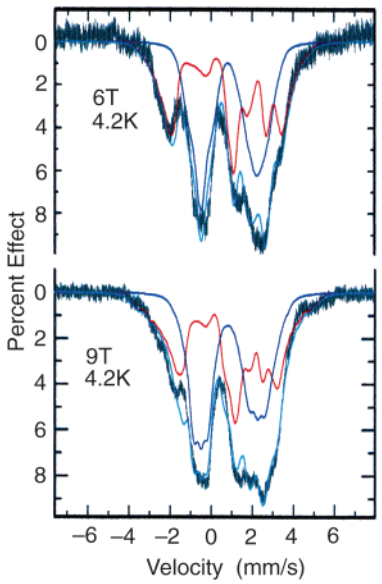

Figure 7. Plots showing the observed Mössbauer spectra in applied magnetic field. The sample was prepared from a crushed single crystal enriched to 95% ^{57}Fe. The calculated fits (Table 5) for molecule **1** (blue line) and molecule **2** (red line) as well as the sum (light-blue line) and experimental data are shown.

Establishing the sign of the quadrupole splitting requires measurements in the applied magnetic field. It is clear that the spectra in the applied magnetic field will be much more difficult to interpret as the deconvolution into the components from the two species will be more complex than those in the near-zero field. To assist in this formidable task, we have required simultaneous fits to the magnetic spectra for measurements under differing conditions (two fields (6 and 9 T) at 4.2 K and at 9 T at three temperatures (100, 200, and 250 K)). Further, we constrained the sign of the zero-field splitting to be negative, as expected for imidazole and imidazolate−ligated complexes,[26,65] and in addition, the absorption areas of the two sites were constrained to be the same. The 4.2 K spectra are assumed to represent the slow-relaxation limit, whereas the higher-temperature spectra are taken to be in the fast-relaxation limit. The fits shown in Figure 7 use a positive sign for the site with larger quadrupole splitting and a negative sign for the other site. Illustrations of the fits of the Mössbauer spectra obtained in a 9 T field at 100 and 250 K are given in the Figure S3 of the

(59) Champion, P. M.; Chiang, R.; Münck, E.; Debrunner, P.; Hager, L. P. *Biochemistry* **1975**, *14*, 4159.
(60) Shaevitz, B. A.; Lang, G.; Reed, C. A. *Inorg. Chem.* **1988**, *27*, 4607.
(61) Bominaar, E. L.; Ding, X.; Gismelseed, A.; Bill, E.; Winkler, H.; Trautwein, A. X.; Nasri, H.; Fisher, J.; Weiss, R. *Inorg. Chem.* **1992**, *31*, 1845.
(62) Nasri, H.; Fischer, J.; Weiss, R.; Bill, E.; Trautwein, A. X. *J. Am. Chem. Soc.* **1987**, *109*, 2549.
(63) Schappacher, M.; Ricard, L.; Fisher, J.; Weiss, R.; Montiel-Montoya, R.; Bill, E. *Inorg. Chem.* **1989**, *28*, 4639.
(64) Schappacher, M.; Ricard, L.; Weiss, R.; Montiel-Montoya, R.; Gonser, U.; Bill, E.; Trautwein, A. X. *Inorg. Chim. Acta* **1983**, *78*, L9.
(65) Perturbation expressions for the ZFS parameters *D* and *E* make this expectation plausible for a ground d_{xy} state in the t_{2g} multiplet with octahedral symmetry. However, a very low symmetry ligand field at the iron site may well mix the t_{2g} states in a way that causes *E*/*D* to approach its maximal rhombic value and thus make the sign of *D* ambiguous. We note that our fits to the spectra resulted in relatively small values for *E*/*D*, which provides some modest support for the consistency of constraining *D* to be negative. Admittedly, *E*/*D* is a soft parameter, in that it could be constrained to a much large value and variation of other fit parameters could converge to a fit of nearly comparable quality.

Table 5. Fits for Applied Field Mössbauer Measurements

complex	molecule **1**	molecule **2**
	δ_{Fe}, mm/s	
4.2 K	0.92	0.97
100 K	0.91	0.96
200 K	0.87	0.91
250 K	0.85	0.89
	ΔE_Q, mm/s	
4.2 K	−2.40	2.90
100 K	−2.30	2.90
200 K	−1.98	2.55
250 K	−1.84	2.38
η	0.90	0.71
D, cm^{-1}	−3.7	−9.8
E/D	0.04	0.01
Γ(mm/s)	0.3	0.3
$A^*_{xx}/g^*_N\beta_N$, T	−20.7	−29.7
$A^*_{xx}/g^*_N\beta_N$, T	−5.4	−16.5
$A^*_{xx}/g^*_N\beta_N$, T	−8.1	−2.8
α^a(D→Q)	−1	5
β^a(D→Q)	−43	−126
γ^a(D→Q)	13	71

[a] Euler angles for rotation of the electric field gradient with respect to the ZFS tensor. See Tinkham, M. Group Theory and Quantum Mechanics; McGraw-Hill Book Company: New York, 1964; p 102.

Supporting Information. A complete set of the values used to obtain these fits is given in Table 5.

Thus, we have shown that a plausible interpretation of these data is that they represent a site with Mössbauer parameters similar to those of a high-spin imidazole-ligated species and a second site with Mössbauer parameters similar to those of a high-spin imidazolate-ligated species. However, with the large number of fit parameters in this two-site model, the set of parameters that result in this fit are certainly not unique. We can at least conclude that a fit with opposite sign of the quadrupole splitting constant for the two distinct iron sites in the crystal is a likely description of the experimental Mössbauer data, even though we cannot absolutely rule out other interpretations. Clarification of this question might be possible with additional data at higher field (not currently available to us) or under lower temperature conditions (to ensure slow relaxation) in a series of fields between 1 and 9 T. Despite the possible ambiguities in the fits to the Mössbauer data, it is clear that, in this system, the presence of a strong hydrogen bond has had a substantial effect on the electronic structure.

Summary

We have described the characterization of the crystalline complex [Fe(TPP)(2-MeHIm)]$_2$·2-MeHIm, which is a high-spin iron(II) porphyrinate species containing two distinct iron sites. Each iron porphyrinate is ligated by a single imidazole ligand, however the imidazole in one site is well separated, whereas the second coordinated imidazole is involved in a strong hydrogen bond to an intermolecular hydrogen bond acceptor. These environmental effects of the axial ligand lead to substantial effects on the geometric structure around iron and most probably on the electronic structure of iron at the two sites. The effect of a strong hydrogen bond to a coordinated imidazole can indeed lead to imidazolate-like properties at iron. One site is best described as closely similar to the active iron site in deoxyhemoglobin and -myoglobin; the second site is imidazolate-like and corresponds more closely to the site found in horseradish peroxidase and other peroxidases.

Acknowledgment. We thank the National Institutes of Health for support of this research under Grant GM-38401 and NSF CHE-0443233 for X-ray instrumentation support. Work at Argonne National Laboratory was supported by the U.S. Department of Energy, Office of Science, Office of Basic Energy Sciences, under contract DE-AC02-06CH11357.

Supporting Information Available: Figure S1 displaying displacements from the 24 atom plane, Figure S2 showing a Mössbauer spectrum at 200 K, and Figure S3 displaying the fits in applied field at 100 and 250 K. Table S1 giving NSD values and Table S2 showing variable temperature Mössbauer quadrupole splitting and isomer shifts for both components. Tables S3−S8, giving complete crystallographic details, atomic coordinates, bond distances and angles, anisotropic temperature factors, and fixed hydrogen atom positions. X-ray and neutron crystallographic files, in CIF format, are available. This material is available free of charge via the Internet at http://pubs.acs.org.

JA078222L